Optics Communications 342 (2015) 230–237

Contents lists available at ScienceDirect

Optics Communications

journal homepage: www.elsevier.com/locate/optcom

Discussion

Analysis of a log periodic nano-antenna for multi-resonant broadband field enhancement and the Purcell factor

Jie Yang, Fanmin Kong*, Kang Li, Shiwei Sheng

School of Information Science and Engineering, Shandong University, No. 27, South Shanda Road, Licheng Street, Jinan 250100, China

ARTICLE INFO

Article history:
Received 13 October 2014
Received in revised form
24 December 2014
Accepted 28 December 2014
Available online 31 December 2014

Keywords:
Log periodic
Nano-antenna
Field enhancement
Purcell factor

ABSTRACT

Broadband nano-antennas play a central role in many areas of science and technology. However, a more intuitive understanding for rational design of nano-antennas with broadband response is desirable. A log periodic nano-antenna was studied in the paper. The finite-difference time-domain method was used to explore the spectral characteristics of the log periodic nano-antenna by the excitation mode of reception and emission. The effects of geometry on field enhancement and the Purcell factor were systematically described and investigated. The field enhancement of the nano-antenna can be tuned by geometric parameters such as the outer radius, the tooth angle, and the ratio of the radial sizes of successive teeth, which provide control over both the spectral resonance position and the field enhancement peak amplitude. The Purcell factor mainly depends on the outer radius, the tooth angle, and the bow angle. In addition, multi-resonant field enhancement was analyzed in detail by conformal transformation. Furthermore, a careful comparison of the characteristics of a bowtie nano-antenna demonstrated that the log periodic nano-antenna has considerable potential for multi-resonant field enhancement and improvement of the Purcell factor. The results provide a promising prospect for designing and optimizing the log periodic nano-antenna in a broad range of wavelengths.

1. Introduction

In the past years, with the advance in nanotechnology, optical antennas have attracted intense research interests due to their ability of converting freely propagating optical radiation into localized energy, and vice versa [1], which results in a large electromagnetic field enhancement in the proximity of the antenna. In addition, they can tailor the excitation and emission processes of nearby fluorescent molecules or quantum dots. Based on these characteristics, optical antennas have great potential for applications in many fields, such as photo detection [2,3], light emission [4], sensing [5], trapping [6], heat generation [7], nano-imaging, and spectroscopy [8]. Top-down nanofabrication tools such as focused ion beam milling or electron-beam lithography and bottom-up self-assembly schemes have been widely used to fabricate prototype nano-antennas. These techniques provide an emerging opportunity for realizing new optoelectronic devices. Many optical antennas have been studied over the past few years, such as the monopole antenna [9–11], particle antenna [12], Yagi-Uda antenna [13,14], gap antenna [15], slot antenna [16], cross antennas [17], and patch antennas [18]. Recently most theoretical studies on optical antennas have been focused on the bow-tie antennas [19] and gap antenna because of their remarkable ability of strongly enhancing and confining optical fields to very small dimensions, surpassing the diffraction limit, and efficiently emitting the near field energy to the far field [20, 21]. However, their operation bandwidths are significantly below an octave. In fact, a broadband nano-antenna plays a central role in many specific applications, such as perfect lensing via phase conjugation and time reversal for enhancing the efficiency of non-linear processes at the fundamental and harmonic frequency. Moreover, nano-antennas with broadband response have made significant contributions in the area of surface-enhanced linear/nonlinear vibrational spectroscopy [22,23] and spontaneous two-photon emission [24,25]. So, designing and optimizing a nano-antenna with a significant amount of bandwidth has become highly desirable.

A way of achieving broadband behavior is to develop an antenna with a self-similarity structure. Furthermore, antenna design with self-similarity is regarded as a promising approach to improve broadband behavior. Recently, a number of antenna designs with self-similarity have been extensively studied, such as self-similar gold-nanoparticle antennas [26], self-similar optical antenna arrays [27], dipole array antennas [28], and fractal abstraction of the plasmonic bowtie antenna [29]. Fractal antennas are

* Corresponding author.
E-mail address: kongfm@sdu.edu.cn (F. Kong).

http://dx.doi.org/10.1016/j.optcom.2014.12.075
0030-4018/© 2015 Published by Elsevier B.V.

generally characterized by broadband or multiband behavior and highly isotropic emission/reception angular patterns. However, the self-similar optical antenna has a very sophisticated structure. A compact advanced design can be found such as the log periodic nano-antenna. Several theoretical and experimental studies of the log periodic nano-antenna have been concerned with broadband directivity and field enhancement [30, 31]. Recently, Navarro-Cia et al. [32] conducted a very significant study of the log periodic nano-antenna. Following Navarro-Cia, we carefully checked the influence of the geometric parameters on field enhancement and extend the optical properties of the log periodic nano-antenna to the Purcell factor. The peculiar properties of the log periodic nano-antenna (LPNA) were investigated with great emphasis on field enhancement and the Purcell factor. At the same time, the characteristics of the nano-antenna were compared with the bowtie nano-antenna (BNA). The analysis may provide a guide for designing and optimizing LPNA with wideband response.

2. Antenna models and computational approach

The nano-antennas geometry is shown in Fig.1. The geometry of the antenna is defined by the following parameters: outer radius R_n, the inner radius r_n, the tooth angle β, the bow angle α, the number of teeth N, the thickness t, and the gap g between the two arms. The ratio of the radial sizes of successive teeth is defined as $\tau = R_n/R_{n+1}$. To account for a realistic environment the LPNA is supported by a silica substrate having permittivity $\varepsilon_{sub} = 2.25$ with thickness $T = 90$ nm and radius $R_s = 583$ nm. The tips of the two circular-toothed structures are rounded off with a radius of curvature of 5 nm. In order to describe the optical response of the LPNA, a modified Drude dielectric function is employed

$$\varepsilon(\omega) = \varepsilon_\infty - \omega_p^2/(\omega^2 + j\omega\gamma), \quad (1)$$

where ε_∞, ω_p, and $1/\gamma$ stand for the dielectric constant for the frequency going to the infinite, the plasmon frequency, and the relaxation time of the metal, respectively. For silver, the parameters used were $\varepsilon_\infty = 4.039$, $\omega_p = 9.154$ eV, and $\gamma = 0.815$ eV [33].

The Purcell factor F used in this paper was formulated [20] in (2) as follows:

$$F = \frac{\iint P(\theta, \varphi) d\Omega}{\iint p_0(\theta, \varphi) d\Omega} \quad (2)$$

where $P(\varphi, \theta)$ and $P_0(\varphi, \theta)$ are the power radiating to the far field for the system studied and for the reference dipole in a vacuum, respectively.

To facilitate the design and final assessment of the performance of the LPNA, finite-difference time-domain [34–36] (FDTD) simulations were performed. In our paper, calculation regions were 2000 nm × 2000 nm × 2000 nm. For modeling, perfectly matched absorbing boundary conditions were introduced in all directions in order to avoid parasitic nonphysical reflection around the structure. The antenna region was set to 6 nm × 4 nm × 5 nm, while the mesh size was 0.5 nm × 1 nm × 5 nm in the zone between the antenna arms. Such dense mesh was required in this region as it possesses rapid variation and maximum concentration of the electromagnetic fields. A uniform mesh was used outside the antenna with a maximum step of 24 nm. In order to investigate spectrum characteristics of field enhancement (i.e., $|E|/|E_{\text{incident}}|$), the nano-antenna was induced by a normal-incident plane-wave polarized in the y-direction, and the nano-antenna was also excited by an electric dipole emitter placed at the gap equidistantly between the two halves of the antenna to analysis Purcell factor characteristics. The electric dipole lay in the same plane as the antenna and was oriented in its longitudinal direction.

3. Results and discussion

The influence of the geometrical parameters of LPNA on the antenna properties were analyzed in the following study. All parameters mentioned above, except for the thickness of the structure, were systematically varied in order to investigate their effects on the field enhancement and the Purcell factor of the nano-antenna.

First, effects of the outer radius of the circular-toothed structure on the field enhancement and the Purcell factor of LPNA were theoretically investigated. Fig. 2(a) shows how the field enhancement changes with different outer radii R of the circular-toothed structure. It can be observed that as R becomes larger from 500 nm to 800 nm, the field enhancement at both resonances is higher. In addition, the resonances move toward longer wavelengths with an increase of the outer radius R. Three obvious peaks and an inconspicuous peak in the field enhancement can be identified for a 3 tooth nano-antenna, which suggest that the number of peaks for the field enhancement is $N+1$, where N is the number of teeth. This result is in accord with the former conclusion drawn by Navarro-Cia [32]. To illustrate the dependence of the Purcell factor on the outer radius, Fig. 2(b) shows the variation of the Purcell factor with the outer radius. It can be seen that the Purcell factor values at resonances increase with the increase of R. In addition, as the outer radius of the circular-toothed structure increases, the

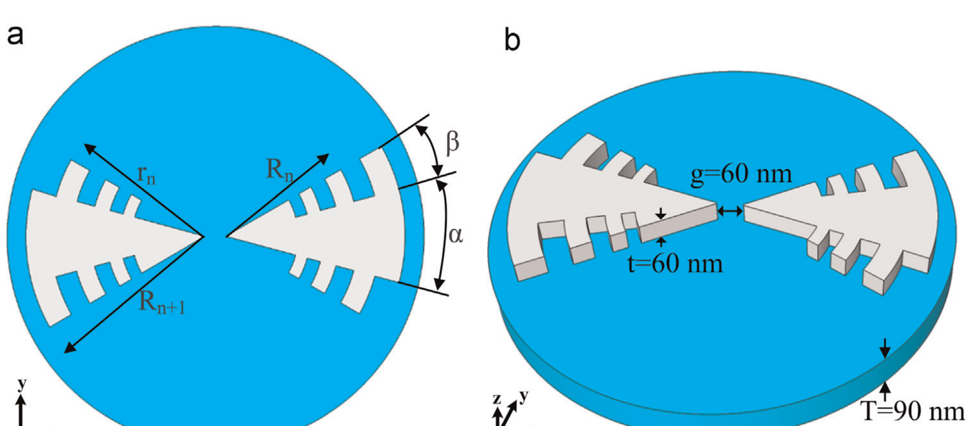

Fig. 1. Log periodic nano-antenna (a) top view and (b) three-dimensional schematic view. Geometric parameters: $t=60$ nm, $g=60$ nm, $T=90$ nm.